On Cattaneo-Christov heat flux analysis with magneto-hydrodynamic and heat generation effects in a Carreau nano-fluid over a stretching sheet

Usman Ali^{a,*}, Ali S. Alqahtani^{b}, Khalil Ur Rehman^{c} and M.Y. Malik^{b}
^{a}*Department of Mathematics, Faculty of Natural Sciences, Quaid-i-Azam University, Islamabad 44000, Pakistan.*
*e-mail: usmanali@math.qau.edu.pk
^{b}*Department of Mathematics, College of Sciences, King Khalid University, Abha 61413, Saudi Arabia.*
^{c}*Department of Mathematics, Air University, PAF Complex E-9, Islamabad 44000, Pakistan.*

This pagination specifies the characteristics of Cattaneo-Christov heat diffusion model for the stagnation point flow of a Carreau nano-fluid. The momentum equation is manifested with magneto-hydrodynamic effect and the generalised Fourier's law and Fick's law are considered to manipulate the heat and mass flux with heat generation and chemical reaction. The fluid flow having infinite shear rate viscosity is caused by the stretched sheet. The admissible transformations are invoked to alter the flow narrating coupled partial differential system into the coupled ordinary differential system. Later on, these equations are sorted out numerically with the aid of Runge-Kutta Fehlberg method supported with shooting scheme. The graphs are plotted that portrays the impact of fluid velocity and temperature towards various engineering parameters which reveals that the fluid temperature increases when enlarging heat generation parameter. The validations for the numerical values of skin friction coefficient are delineated with the existing literature. Also, the numerical findings for the local Nusselt number are offered.

Keywords: Carreau nano-fluid; stagnation point flow; chemical reaction; Cattaneo-Christov heat flux model; heat generation.

1. Introduction

In the past few decades, researchers are interested in several aspects of the non-Newtonian fluid which represents the non-linear relation between shear stress and shear rate. The flow diversity of non- Newtonian fluid model leads to uncertainty related to rheological features. One cannot explain the complete phase through single constitutive equation which establish the relation between deformation rate and shear stress. Shear thinning is the non-Newtonian behaviour of fluids whose viscosity decreases under shear strain. The non-Newtonian behaviour of fluids are of huge importance because of its usage at industrial and technological scales such as melting of polymers, paints, asphalts and glues. In view of its importance, many recent studies have been found on the flow of Newtonian and non-Newtonian fluids. One of the most commonly used rheological model and has certain advantages over non-Newtonian fluid models. Further, non-Newtonian flows from wedge phenomena arise in a number of chemical engineering systems. The Carreau (1972) viscosity model is known to be a good approximation for a large number of shear-thinning fluids due to its capability to catch the rheological behaviour at very low and very high shear rates, while other idealized models, like the widely used Ostwald de Waele power-law model, are valid only in a limited range of operational conditions. An analysis is carried out in order to highlight the importance of boundary layer flow in various industrial applications such as the condensation process of metallic plate in a cooling bath and glass, extrusion of plastic sheets, aerodynamic and also polymer industries. Mehta and Rao [1] had given the remarkable conclusions about non-Newtonian fluids in a porous medium past a verti-

cal flat plate with non-uniform surface heat flux. Pascal and Pascal [2] give their analysis on non-Newtonian fluids along with some non-linear shear flows. Pressure drop through porous media in non-Newtonian purely viscous fluid flow examined by Sabiri and Comiti [3]. Some later works on the boundary layer flow of non-Newtonian fluids are presented in Refs. [4-10]. Etemad [11] explored the non-Newtonian fluid flow and heat transfer in three dimensional laminar phenomena. In case of ducts and porous media, Liu and Masliyah [12] gave their analysis on non-Newtonian fluid flow. Turbulent flow in a membrane tube with mass transfer in Newtonian and non-Newtonian fluids studied by Parvatiyar [13]. Slip-flow boundary conditions for non-Newtonian lubrication layers has been studied by Anderson and Valnes [14]. Also, some useful applications regarding non-Newtonian flow is observed by Hoyt [15]. Papalexandris [16] elaborates the study of wedge-induced detonations in numerical aspects. The theme beyond the flow of viscous incompressible fluid with thermal conductivity and temperature dependent viscosity past a permeable wedge aside by uniform surface heat flux is studied by Hossain *et al.* [17]. In Carreau model, fall of non-spherical particles in a liquid is studied by Machac *et al.* [18]. Moreover, various aspects regarding Carreau fluid models are investigated in Refs. [19-25]. The effects of peristaltic transport with magnetic field in a Carreau fluid is reported by Hayat *et al.* [26]. A numerical analysis is carried out upon sheardependent non-Newtonian fluids in compliant vessels reported by Hundertmark-Zauskova and Lukacova-Medvid'ova [27].

The Fourier laws are used frequently, to determine the characteristics of heat transfer phenomena. Cattaneo-Christov heat flux model is the rectified form of the Fourier

law which is used to determine the specifications of heat flux model. A useful results regarding thermal convection in a Newtonian fluid with Cattaneo-Christov heat flux equations are explored by Straughan [28]. He observed that thermal relaxation parameter is notable as Cattaneo number increases Also, Straughan extended his work by considering the Cattaneo-Christov heat flux model in transverse waves [29]. Cattaneo equations with thermal stratification are analysed and their closed form solutions are discussed by Al-Qahtani and Yilbas [30]. The Cattaneo-Christov heat flux is applied to Newtonian fluids and uniqueness solutions are discussed by Tibullo and Zampoli [31]. The analytical solutions of thermal slip effects of a Maxwell fluid along with Cattaneo-Christov heat diffusion are discussed by Han *et al.* [32]. Also, the effects of elasticity, slip coefficient, and Prandtl number are shown through graphical representation. Haddad [33] examined the heat flux in a Brinkman porous channel embedded with fluid inertia. Shivakumara *et al.* [34] observed the thermal convection with Cattaneo effects in the solid and found that its impacts on the nature of convective instability are efficient. Mustafa *et al.* [35] studied the rotating flow upon linearly stretching disk. Nanofluids are taken into account to determine the behaviour of heat transfer rate through Cattaneo-Christov heat diffusion formula. Various specifications of Cattaneo-Christov heat flux model are discussed by Hayat *et al.* [36-37]. The characteristics of heat flux through Cattaneo-Christov model in a porous stretching sheet is analysed by Nadeem and Muhammad [38]. The Cattaneo-Christov model with non-Newtonian fluids through stretching regimes is carried out by Abbasi and Shehzad [39]. A theoretical approach for Cattaneo-Christov model embedded with different geometries are observed by Reddy *et al.* [40]. Li *et al.* [41] examined the heat flux for magneto-hydrodynamic (MHD) viscoelastic fluid through stretching sheet. Here, the energy equation have been obtained with the help of Cattaneo-Christov theory. Ramzan *et al.* [42] observed the homogenous-heterogeneous reactions for the third grade fluid merged with Cattaneo-Christov heat flux model. The specifications of heat transfer via Cattaneo-Christov model induced by a stretching cylinder is studied by Malik *et al.* [43]. The numerical scheme for Williamson fluid is discussed and Cattaneo-Christov model is applied to extract the characteristics of heat transfer Salahuddin *et al.* [44]. The heat conduction via Cattaneo-Christov heat flux through parallel plates in the presence of MHD is observed by Dogonchi and Ganji [45]. Upadhya *et al.* [46] studied the Cattaneo-Christov heat flux on time dependent fluids with MHD effects. The numerical approach for MHD fluid flow induced by a cone emerged with Cattaneo-Christov heat flux model is examined by Kumar *et al.* [47]. Further, the importance of Cattaneo-Christov heat diffusion is highlighted in Refs. [48-51].

As the heat conduction laws given by the French mathematician named Jean-Baptiste Joseph Fourier (1768-1830) have been used to investigate the heat transfer mechanism since two centuries in suitable conditions. Later on it was

analysed that this law is not applicable in the case when the initial state is disturbed because it affects the whole system. To overhaul this problem, Cattaneo (1911-1979) had played his role to modify the Fourier law to get the hyperbolic equation by invoking thermal relaxation time. The above literature tells us that no work is done on Cattaneo-Christov heat diffusion model with heat generation and chemical reaction in concern with the motion of the Carreau nano-fluid. To fill the gap, this report is presented in order to ascertain the heat and mass flux rate through Cattaneo-Christov heat and mass diffusion formulas. In Sec. 1, the relevant literature survey is presented in order to enhance the importance of current work. In Sec. 2, the flow describing equations are modelled mathematically and the numerical technique *i.e.* Runge-Kutta Fehlberg method along with shooting scheme is applied to sort out the governing partial differential equations in Sec. 3. The impacts of various physical parameters upon fluid velocity, temperature and concentration are presented through graphs. Also, the numerical values for the skin friction coefficient and local Nusselt number are offered in Sec. 4. In Sec. 5, the results and discussion for the impacts of aforementioned physical parameters are exhibited. Finally, the concluding remarks are done in Sec. 6.

2. Mathematical formulation

The beauty of mathematics allows us to express the upper-convective material derivative for any vectors as follows.

$$\frac{DA}{Dt} = \frac{\partial A}{\partial t} + \vec{V} \cdot \vec{\nabla}A - A \cdot \vec{\nabla}\vec{V} + (\vec{\nabla})A, \qquad (1)$$

where $\vec{V}$ is the velocity vector and A is supposed to be vector form of heat and mass flux. This report is concerned with the Cattaneo-Christov model which specifies the thermal and concentration diffusion. Then the structure in different generalised version of Fourier's law and Ficks's law considering the Cattaneo-Christov form as Refs. [48-51]

$$q + \lambda_H \left[\frac{\partial q}{\partial t} + \vec{V} \cdot \vec{\nabla}q - q \cdot \vec{\nabla}\vec{V} \right.$$
$$\left. + (\vec{\nabla} \cdot \vec{V})q \right] = -k_f \vec{\nabla}T, \qquad (2)$$

$$J + \lambda_M \left[\frac{\partial J}{\partial t} + \vec{V} \cdot \vec{\nabla}J - J \cdot \vec{\nabla}\vec{V} \right.$$
$$\left. + (\vec{\nabla} \cdot \vec{V})J \right] = -D_B \vec{\nabla}C, \qquad (3)$$

where normal heat and mass flux are denoted by q and J, k_f is the thermal conductivity, D_B is the Brownian diffusion, λ_H and λ_M are the relaxation time of heat flux and mass flux. It is important to note down that $\lambda_H = 0$ and $\lambda_M = 0$ lead (2) and (3) to classical Fouriers law and Fick's law, respectively. Now by inserting the condition for incompressible fluids *i.e.* $\nabla \cdot V = 0$ and steady state clause $\partial q/\partial t = 0$, $\partial J/\partial t = 0$,

we get the new form of (2) and (3) as

$$q + \lambda_H[\vec{V} \cdot \vec{\nabla}q - q \cdot \vec{\nabla}\vec{V}] = -k_f\vec{\nabla}T, \qquad (4)$$

$$J + \lambda_M[\vec{V} \cdot \vec{\nabla}J - J \cdot \vec{\nabla}\vec{V}] = -D_B\vec{\nabla}C, \qquad (5)$$

later on we will deduce the energy and mass equations with the help of Eq. (4) and (5). Consider the boundary layer flow for an incompressible Carreau fluid model impinged on a stretching surface where the flow is launched by the stretched sheet. The coordinate system is designed in a way that x-axis is taken to be along stretching sheet whereas y-axis is perpendicular to the sheet and the fluid overcomes at $y > 0$. The uniform magnetic field B_0 is invoked along y-direction whereas the induced magnetic field B_0 is supposed to be negligible for lesser magnetic Reynold's number. The sheet velocity is considered as $u_w(x) = cx$ with $c > 0$ as stretching rate and the exterior velocity as $u_\infty = ax$ where a is con-

stant. The constitutive equations for the generalized Carreau model are taken as

$$\hat{\tau} = -pI + \mu(\dot{\gamma})A_l,$$

$$\mu = \mu_0\left[\beta * + (1 - \beta*)[1 + (\Gamma\dot{\gamma})^2]\right]^{(n-1)/2}, \qquad (6)$$

where $\hat{\tau}$ is the Cauchy stress tensor, p is the pressure, I is the identity tensor, $A_1 = (gradV) + (gradV)^T$ the first Rivlin Erickson tensor, $\dot{\gamma} = \sqrt{(1/2)\Pi}$ with Π as a second invariant strain tensor and defined as $\Pi = trace(A_1^2)$, n the power law index, Γ a material time constant and $\beta* = (\mu_\infty/\mu_0)$ the viscosity ratio parameter with μ_0, the zero shear rate viscosity and μ_∞ the infinite shear rate viscosity and taken to be less than one here.

By manipulating the above assumptions and usual boundary layer approximations, the governing equations for current problem are given as

$$\frac{\partial u}{\partial x} + \frac{\partial v}{\partial y} = 0, \tag{7}$$

$$u\frac{\partial u}{\partial x} + v\frac{\partial u}{\partial y} = u_\infty\frac{du_\infty}{dx} + v\left(\frac{\partial^2 u}{\partial y^2}\right)\left[\beta^* + (1-\beta^*)\left\{1 + \Gamma^2\left(\frac{\partial u}{\partial y}\right)^2\right\}^{(n-1)/2}\right]$$

$$+ v(1-\beta^*)\Gamma^2\left(\frac{\partial^2 u}{\partial y^2}\right)\left(\frac{\partial u}{\partial y}\right)^2(n-1)\left\{1 + \Gamma^2\left(\frac{\partial u}{\partial y}\right)^2\right\}^{(n-3)/2} + \frac{\sigma B_0^2}{\rho}(u_\infty - u), \tag{8}$$

$$u\frac{\partial T}{\partial x} + v\frac{\partial T}{\partial y} + \lambda_H\left(u\frac{\partial u}{\partial x}\frac{\partial T}{\partial x} + v\frac{\partial v}{\partial y}\frac{\partial T}{\partial y} + u\frac{\partial v}{\partial x}\frac{\partial T}{\partial y} + v\frac{\partial u}{\partial y}\frac{\partial T}{\partial x} + 2uv\frac{\partial^2 T}{\partial x\partial y} + u^2\frac{\partial^2 T}{\partial x^2} + v^2\frac{\partial^2 T}{\partial y^2}\right) = \alpha_f\frac{\partial^2 T}{\partial y^2}$$

$$+ \tau\left(D_B\frac{\partial C}{\partial y}\frac{\partial T}{\partial y} + \frac{D_T}{T_\infty}\left(\frac{\partial T}{\partial y}\right)^2\right) + \frac{Q_0}{\rho c_p}(T - T_\infty), \tag{9}$$

$$u\frac{\partial C}{\partial x} + v\frac{\partial C}{\partial y} + \lambda_M\left(u\frac{\partial u}{\partial x}\frac{\partial C}{\partial x} + v\frac{\partial v}{\partial y}\frac{\partial C}{\partial y} + u\frac{\partial v}{\partial x}\frac{\partial C}{\partial y} + v\frac{\partial u}{\partial y}\frac{\partial C}{\partial x} + 2uv\frac{\partial^2 C}{\partial x\partial y} + u^2\frac{\partial^2 C}{\partial x^2} + v^2\frac{\partial^2 C}{\partial y^2}\right) = D_B\frac{\partial^2 C}{\partial y^2}$$

$$+ \frac{D_T}{T\infty}\frac{\partial^2 T}{\partial y^2} - K_0(C - C_\infty), \tag{10}$$

where $\alpha_f = k_f/(\rho c_p)_f$, $\tau = (\rho c)_s/(\rho c)_f$, Q, K are the thermal diffusivity with $(\rho c_p)_f$ as the effective heat capacity of the fluid, ratio of nanoparticle heat capacity and the base fluid heat capacity, heat generation rate, and chemical reaction rate. The boundary conditions are

$$u=u_w=cx, \quad v=0, \quad T=T_w \quad \text{at} \quad y = 0,$$

$$u=u_\infty\to ax, \quad T\to T_\infty \quad C\to C_\infty \quad \text{as} \quad y\to\infty, \quad (11)$$

The following dimensionless quantities are used to change the governing partial differential equations into scheme of ordinary differential equations.

$$\eta = y\sqrt{\frac{c}{v}}, \quad \psi(x,y) = x\sqrt{cv}f(\eta),$$

$$\theta(\eta) = \frac{T - T_\infty}{T_w - T_\infty}, \quad \phi(\eta) = \frac{C - C_\infty}{C_w - C_\infty}, \quad (12)$$

where ψ is to notify as stream functions which is supposed to be satisfied by the continuity equations with $u = \partial\psi/\partial y$ and $v = -\partial\psi/\partial x$. By using the above transformations, the momentum and energy and mass equations with the concerned boundary conditions are

$$[\beta^* + (1-\beta^*)\{1 + We^2(f'')^2\}^{(n-3)/2}\{1 + nWe^2(f'')^2\}]f'''$$

$$+ ff'' - (f')^2 + \alpha^2 + M^2(\alpha - f') = 0, \tag{13}$$

$$\frac{1}{\Pr}\theta'' + f\theta' + N_b\theta'\phi' + N_t(\theta')^2 - \delta_e(ff'\theta' + f^2\theta'')$$

$$+ \gamma\theta = 0, \tag{14}$$

$$\phi'' + Le\Pr f\phi' + \frac{N_t}{N_b}\theta'' - Le\Pr\delta_c(ff'\phi' + f^2\phi'')$$

$$- Le\delta\phi = 0, \tag{15}$$

here,

$$\alpha = \frac{a}{c}, \quad M^2 = \frac{\sigma B_0^2}{\rho c}, \quad We^2 = \Gamma^2 \frac{c^3 x^2}{\upsilon}$$

$$\Pr = \frac{\upsilon}{\alpha_f}, \quad N_b = \frac{\tau D_B}{\upsilon}(C_w - C_\infty),$$

$$N_t = \frac{\tau D_T}{\upsilon T_\infty}(T_w - T_\infty), \quad \delta_e = c\lambda_H, \quad \delta_c = c\lambda_M,$$

$$Le = \frac{\alpha_f}{D_B} \quad \gamma = \frac{Q_0}{\rho C_p}\left(\frac{\upsilon}{c}\right) \quad \text{and} \quad \delta = \frac{K_0}{cx^2}$$

are the velocity ratio parameter, magnetic field parameter, Weissenberg number, Prandtl number, Brownian diffusion coefficient, thermophoresis parameter, temperature relaxation time parameter, nanoparticle volume fraction, Lewis number, heat generation parameter and chemical reaction parameter.

The corresponding boundary conditions are as follows:

$$f(\eta) = 0, \quad f'(\eta) = 1, \quad \theta(\eta) = 1, \phi(\eta) = 1 \text{ at } \eta = 0,$$

$$f'(\eta) \to \alpha, \quad \theta(\eta) \to 0, \quad \phi(\eta) \to 0 \quad \text{as} \quad \eta \to \infty. \quad (16)$$

The involved physical quantities of engineering are skin friction coefficient and local Nusselt number and is defined as

$$C_{fx} = \frac{2\tau_w}{\rho u_w^2(x)}, \quad Nu_x = \frac{xq_w}{k(T_w - T_\infty)}, \quad (17)$$

where τ_w is the surface shear stress and q_w the surface heat flux given by

$$\tau_w = \mu_0 \left(\frac{\partial u}{\partial y}\right)\left[\beta^* + (1-\beta^*)\left\{1 + \Gamma^2\left(\frac{\partial u}{\partial y}\right)^2\right\}^{(n-1)/2}\right]$$

$$q_w = -k(T_w - T_\infty)\sqrt{\frac{u_0}{x\upsilon}}\theta'(0), \quad (18)$$

the dimensionless form of the local skin friction coefficient and the local Nusselt number are defined as:

$$\text{Re}^{1/2}C_{fx} = f''(0)[\beta^* + (1-\beta^*)\{1 + We^2(f''(0))^2\}^{(n-1)/2}],$$

$$\text{Re}^{-1/2}Nu_x = -\theta'(0), \quad (19)$$

where $\text{Re}_x = xu_w/\upsilon$ is the Reynolds number.

3. Computational algorithm

The governing equations Eqs. (11)-(13) are highly nonlinear in coupled form. The shooting algorithm with fourth-fifth order Runge-Kutta integration scheme is proposed in order to get the solution of this system. In this regard, we consider the following steps as follows:

$$f''' = \frac{-\alpha^2 + (f')^2 - ff'' - M^2(\alpha - f')}{[\beta^* + (1-\beta^*)\{1 + nWe^2(f'')^2\}\{1 + We^2(f'')^2\}^{(n-3)/2}]}, \quad (20)$$

$$\theta'' = -\frac{(f\theta' + N_b\theta'\phi' + N_t(\theta')^2 - \delta_e ff'\theta' + \gamma\theta)}{\left(\frac{1}{\Pr} - \delta_e f^2\right)}, \quad (21)$$

$$\phi'' = -\frac{\left(Le\Pr f\phi' + \frac{N_t}{N_b}\theta'' - Le\Pr\delta_c ff'\phi' - Le\delta\phi\right)}{(1 - Le\Pr\delta_c f^2)}. \quad (22)$$

The above set of higher order differential equations descend to a set of first order ordinary differential equations, we introduce new variables as follows.

$$y_1 = f, \quad y_2 = y_1' = \frac{df}{d\eta}, \quad y_3 = y_2' = \frac{d^2f}{d\eta^2},$$

$$y_5 = y_4' = \frac{d\theta}{d\eta}, \quad y_6 = \phi, \quad y_7 = y_6' = \frac{d\phi}{d\eta}, \quad (23)$$

by substituting these expressions, we get

$$y_1' = y_2$$

$$y_2' = y_3$$

$$y_3' = \frac{y_2^2 - y_1 y_3 - \alpha^2 - M(\alpha - y_2)}{\beta^* + (1-\beta^*)[1 + nWe^2 y_3^2]^{(n-3)/2}}$$

$$y_4' = y_5$$

$$y_5' = -\frac{(y_1 y_5 + N_b y_5 y_7 + N_t y_5^2 - \delta_e y_1 y_2 y_5 + \gamma y_4)}{\left(\frac{1}{\text{Pr}} - \delta_c y_1^2\right)}$$

$$y_6' = y_7$$

$$y_7' = -\frac{\left(Le\text{Pr}y_1 y_7 - \frac{N_t}{N_b}y_5' - Le\text{Pr}\delta_c y_1 y_2 y_7 - Le\delta y_6\right)}{(1 - Le\text{Pr}\delta_c y_1^2)} \tag{24}$$

the transformed boundary conditions are

$$y_1(\eta) = 0, \quad y_2(\eta) = 1, \quad y_4(\eta) = 1, \quad y_6(\eta) = 1 \text{ at } \eta = 0,$$

$$y_2(\eta) \to \alpha, \quad y_4(\eta) \to 0, \quad y_6(\eta) \to 0 \text{ as } \eta \to \infty, \tag{25}$$

the initial guesses for the values of $f''(0)$, $\theta'(0)$ and $\phi'(0)$ are $y_3(0) = u_1$, $y_5(0) = u_2$, $y_7(0) = u_3$.

The following procedure is done in order to solve the above system of equations by shooting method:

- Firstly, choose the values of η_∞ between 5 and 10.

- Then we pursue the initial guesses for $y_3(0)$, $y_5(0)$ and $y_7(0)$. Initially, $y_3(0) = y_5(0) = y_5(0) = 1$ are adopted.

- Then we sort out the ODE's by considering fourth-fifth order Runge-Kutta technique.

- Finally, the absolute variations in the given and calculated values of $y_3(\infty)$, $y_5(\infty)$, and $y_7(\infty)$ that is boundary residuals are calculated. The solution is said to be convergent if it lies below the tolerance error, which is considered to be 10^{-5}.

4. Graphical representation

FIGURE 2. Influence of β^* on $f'(\eta)$ for $\alpha = 1$.
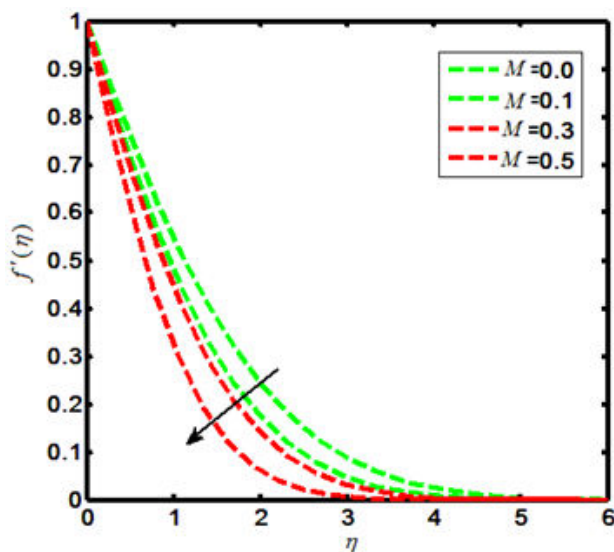
FIGURE 1. Influence of M on $f'(\eta)$ for $\alpha = 0.01$.
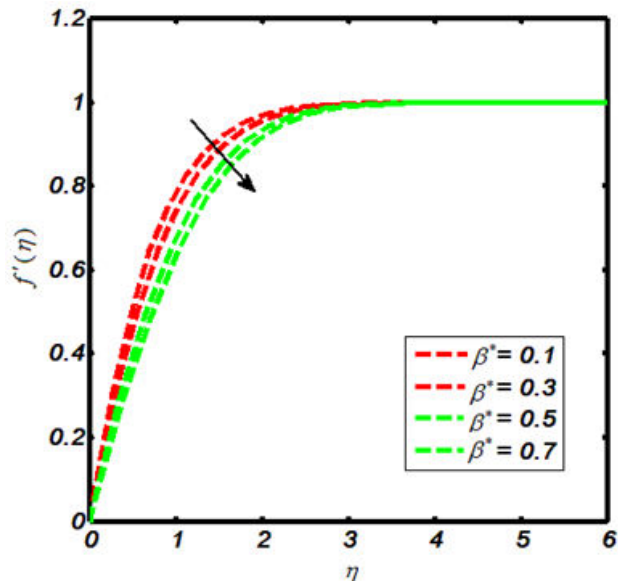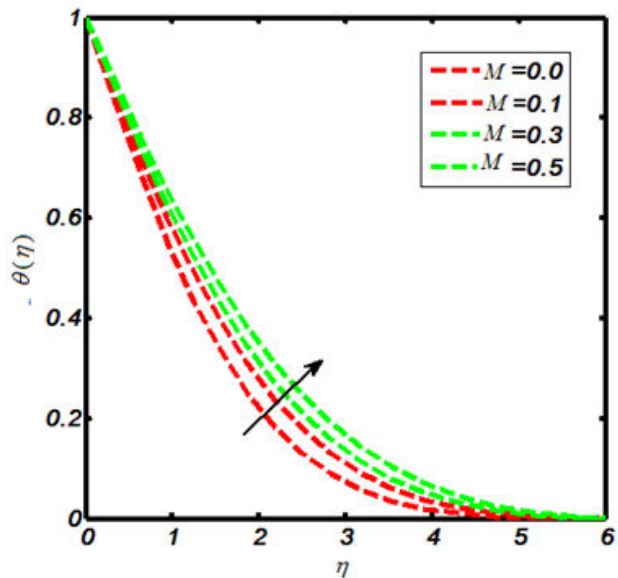
FIGURE 3. Influence of M on $\theta(\eta)$.
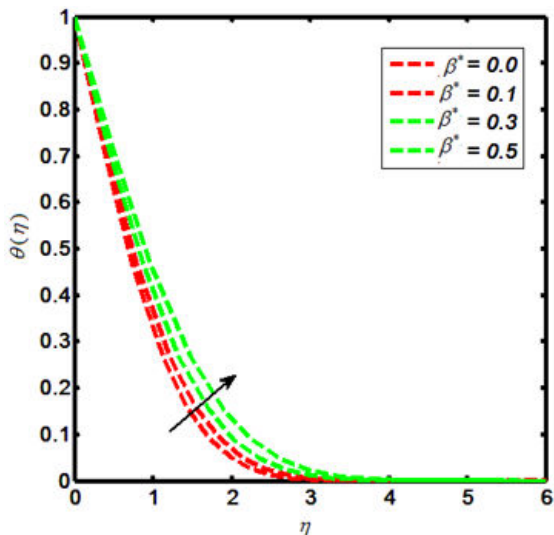
FIGURE 4. Influence of β^* on $\theta(\eta)$.
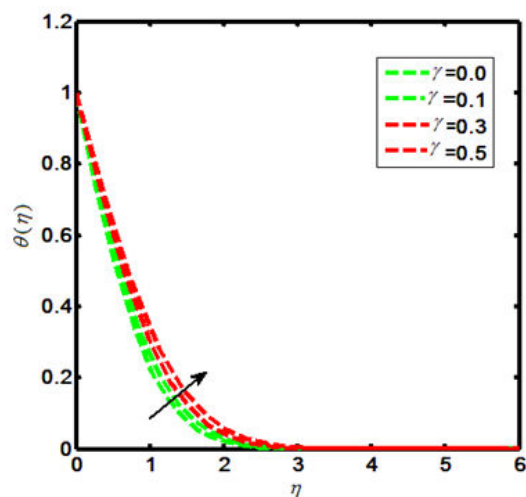
FIGURE 7. Influence of γ on $\theta(\eta)$.
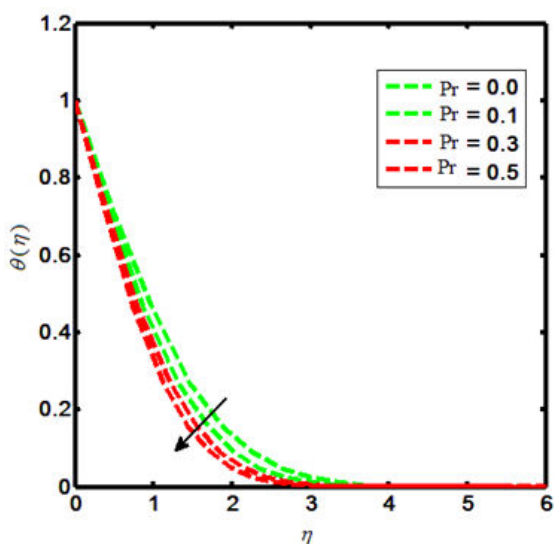
FIGURE 5. Influence of Pr on $\theta(\eta)$.
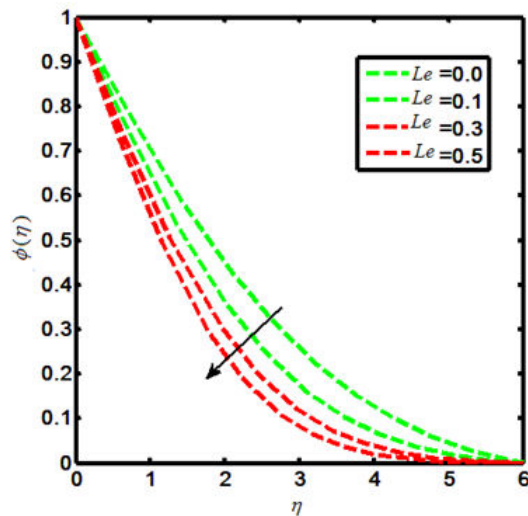
FIGURE 8. Influence of Le on $\phi(\eta)$.
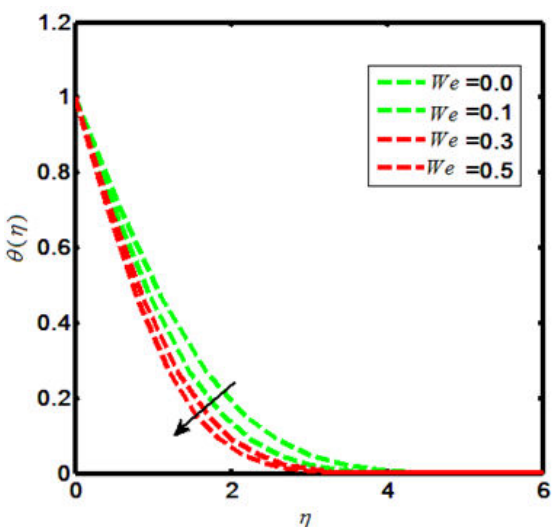
FIGURE 6. Influence of We on $\theta(\eta)$.
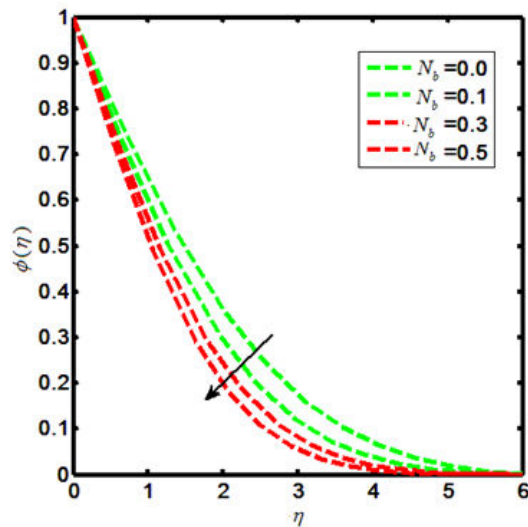
FIGURE 9. Influence of N_b on $\phi(\eta)$.
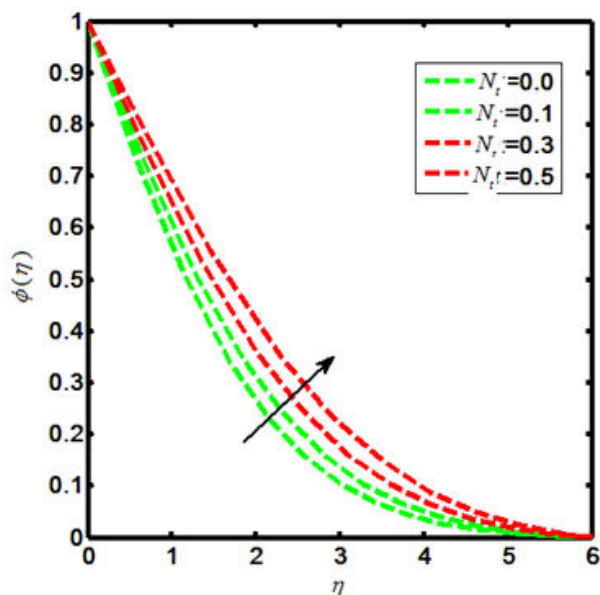
FIGURE 10. Influence of N_t on $\phi(\eta)$.

5. Results and discussion

The Carreau nano-fluid with stagnation point flow towards a stretching sheet is debated in the present report. The Carreau nano-flow model is manifested with externally applied magnetic field. The energy and mass equations are presumed by the Cattaneo-Christov heat and mass flux model. The thermal boundary layer is executed with heat generation and chem-

ical reaction. The laws of conversation of momentum and energy are used to describe the flow field that can be shown in the form of coupled partial differential equations. Later on, such equations are further reformed to coupled ordinary differential equations by declining the independent variables. The similarity transformation is considered in order to reduce the number of independent variables. The numerical results for the reduced system are sorted out by means of shooting technique with Runge-Kutta Fehlberg method. The involved physical parameters are M (magnetic field parameter), β^* (viscosity ratio parameter), N_B (Brownian motion parameter), N_t (thermophoresis parameter), γ (heat generation parameter). The impacts of both the M and β^* on the Carreau fluid velocity are investigated and provided by means of Figs. 1-2. Further, the influences of M, β^*, Pr, We and γ on the Carreau fluid temperature are explored and the results in this context are presented in Figs. 3-7. Also, the fluctuation in Carreau fluid concentration towards Le, N_b and N_t is acquired and shown in the form of Figs. 8-10. Now in detail, Fig. 1 indicates the influence of M on Carreau fluid velocity. It is testified that the fluid velocity shows the decline values towards M when $M(= 0.0, 0.1, 0.3, 0.5)$ and this is due to the fact that increasing the values of M causes the enhancement of Lorentz force. This is a kind of resistive force that oppose fluid particles to move in a free manner and as result the average velocity of the Carreau fluid gets diminished. The influence of β^* on a Carreau fluid velocity is observed and the fluctuation in this regard is captured in Fig. 2. When we iterate $\beta^*(= 0.1, 0.3, 0.5, 0.7)$, the velocity profile declines. The Carreau fluid temperature relies upon the variation of M, β^*, Pr, We, γ. To be more specific, the effects of M on a Carreau

TABLE I. The numerical values for the skin friction in comparison with [52].

M	We	α	β^*	$-(1/2)\sqrt{Re}C_{fx}$	Current results
				$n = 1.75$	$n = 1.75$
0	3	0.3	0.001	-1.053800	-1.0537
0.3	3	0.3	0.001	-1.090060	-1.0901
0.6	3	0.3	0.001	-1.194930	-1.1954
0.8	3	0.3	0.001	-1.298290	-1.29830
0.3	2	0.3	0.001	-1.012570	-1.0126
0.3	3	0.3	0.001	-1.090060	-1.0901
0.3	3.5	0.3	0.001	-1.125350	-1.1252
0.3	4	0.3	0.001	-1.158450	-1.1586
0.3	3	0.7	0.001	-1.090060	-1.0901
0.3	3	1.3	0.001	-0.490977	-0.4910
0.3	3	0.3	0.001	0.598867	0.5989
0.3	3	0.7	0.001	1.827620	1.8277
0.3	3	1.3	0.001	-1.090210	-1.0901
0.3	3	1.7	0.001	-1.059190	-1.0592
0.3	3	0.3	0.0	-1.024390	-1.0244
0.3	3	0.3	0.2	-1.007155	-1.0073

TABLE II. The numerical values of local Nusselt number $(-\theta'(0))$ towards various values of Pr, N_t and N_b.

Pr	N_t	N_b	$Re^{-1/2}Nu_x = -\theta'(0)$
1.0	0.2	0.3	0.31492
1.0	0.2	0.3	0.2141
1.0	0.2	0.3	0.2765
1.0	0.2	0.3	0.3166
3.0	0.3	0.3	0.3234
3.0	0.3	0.3	0.2902
3.0	0.3	0.3	0.2861
3.0	0.3	0.3	0.2397
5.0	0.5	0.3	0.2921
5.0	0.5	0.3	0.3327
5.0	0.5	0.3	0.2690

fluid temperature is inspected and the results are presented in the form of Fig. 3. The enhancing values of causes uplift in the Carreau fluid temperature. Figure 4 indicates the fluctuation in Carreau fluid temperature due to β^* and thus testifies that the temperature enlarges as $\beta^*(= 0.1, 0.3, 0.5, 0.7)$. Figures 5-6 show the impacts of Pr and We upon Carreau fluid temperature. This presents the picture of temperature profile getting decline towards $Pr = (0.0, 0.1, 0.3, 0.5)$ and $We = (0.0, 0.1, 0.3, 0.5)$. Figure 7 is prepared to describe the link between heat generation and Carreau fluid temperature. On iterating the values of γ *i.e.* $\gamma(= 0.0, 0.1, 0.3, 0.5)$, one can observe that Carreau fluid temperature enhances. This is due to the fact that the production of heat energy emits heat particles that causes increase in temperature. The influence of Carreau fluid concentration towards Le is offered in Fig. 8. This picture shows the decaying trend for Carreau fluid concentration towards $Le(= 0.0, 0.1, 0.3, 0.5)$. Figure 9 depicts the fluctuation in the fluid concentration corresponding to multiple values of Brownian motion parameter N_b. The larger values of $N_b(= 0.0, 0.1, 0.3, 0.5)$ causes reduction in the fluid concentration as well as the related boundary layer thickness. This is because of the Brownian force confined the fluid particles to move in the reverse direction of the concentration gradient and causes the fluid more consistent. Thus, the uplifting values of N_b causes the lower concentration gradient and more uniform concentration profile. Figure 10 delineated the impacts of N_t on the Carreau fluid concentration $\phi(\eta)$. Here the fluid concentration and the corresponding boundary layer thickness increases for higher values of N_t *i.e.* $N_t(= 0.0, 0.1, 0.3, 0.5)$. Physically the thermophoretic force implies to oppose the nanoparticles against the direction of temperature gradient. This may also cause the nano-particles in a fluid concentration to be more non-unifrom. Thus the concentration gradient enhances for large values of N_t and causes for more non-uniform fluid concentration. The variation of skin friction coefficient corresponding to various values of M, We, α and β^* are shown in Table I. It is testified that excellent match is captured for current results with the existing literature [52]. Also, the numerical values for the local Nusselt number towards various values of Pr, Nt and N_b are delineated in Table II.

6. Concluding remarks

The current report elaborates the specification of Cattaneo-Christov heat diffusion formula merged with the Carreau nano-fluid flow at a stagnation point. The energy and mass equations are manifested with heat generation and chemical reaction whereas the flow is caused by the stretching sheet. The governing PDE's descend to ODE's through similarity transformations. The numerical results are deduced with the aid of Runge-Kutta Fehlberg technique with shooting proficiency. The numerical findings for the skin friction coefficient and the local Nusselt number are deduced. The key points are as follows:

- The Carreau fluid velocity trend is observed as declined towards M.

- The higher values of β^* causes the decreasing trend for Carreau velocity profile.

- The Carreau fluid temperature enhances corresponding to higher values of M.

- It is observed that the Carreau fluid temperature increases by uplifting β^* and γ .

- The temperature trend for the Carreau fluid model testifies the decline towards Pr and We.

- The Carreau fluid concentration profile decreases for growing values of Le.

- The investigation tells us that Carreau concentration trend diminish when enlarging N_b.

- On uplifting the values of N_t, we get the increasing trend for Carreau concentration profile.

Nomenclature

u, v	Velocity component in $x-$, $y-$directions (m/s)
x	Direction along the surface (m)
y	Direction normal to the surface (m)
T	Temperature of the fluid (K)
T_w	Temperature at sheet (K)
μ	Dynamic viscosity (Ns/m^2)
c_p	Specific heat capacity at constant pressure (J/ KgK)
λ_H	Relaxation time of heat flux
k_f	Thermal conductivity (W/mK)
$(\rho c_p)_f$	Effective heat capacity (Kg/ m^{3}K)
T_∞	Temperature away from the sheet (K)
ρ	Density of the fluid (Kg/m^3)
D_B	Brownian diffusion coefficient
$N_b = \frac{\tau D_B(C_w - C_\infty)}{v}$	Brownian motion parameter
$\delta_\epsilon = c\lambda_H$	Relaxation time parameter of temperature
$\alpha_f = \frac{k_f}{(\rho c_p)_p}$	Coefficient for thermal diffusion (m^2/s)
$f'(\eta)$	Dimensionless velocity
$\phi(\eta)$	Dimensionless temperature
σ	Electrical conductivity
q	Heat flux
$Le = \frac{\alpha_f}{D_B}$	Lewis number
$\delta_c = c\lambda_M$	Nano-particle volume fraction
Γ	Material time constant
$M^2 = \frac{\sigma B_o^2}{\rho c}$	Magnetic field parameter
v	Kinematic viscosity (m^2/s)
γ, δ	Dimensionless parameter
η	Similarity variable
k_o	Reaction rate
$\mathrm{Re}_x = \frac{x u_w}{v}$	Reynold number
$\tau = \frac{(\rho c)_s}{(\rho c)_f}$	Ratio of nanoparticles heat capacity and the base fluid heat capacity
q_w	Surface heat flux
τ_w	Surface shear stress
D_T	Thermophoresis diffusion coefficient
$N_t = \frac{\tau D_T(T_w - T_\infty)}{v T_\infty}$	Thermophoresis parameter
$\beta^* = \frac{\mu_\infty}{\mu_s}$	Viscosity ratio parameter
$u_\infty = ax, \ (a > 0)$	Velocity of exterior flow
$\alpha = \frac{a}{c}$	Velocity ratio parameter
$We^2 = \frac{c^3 \Gamma^2 x^2}{v}$	Weissenberg number
$\mu_0, \ \mu_\infty$	Zero and infinite shear rate viscosity
$Pr = \frac{v}{\alpha_f}$	Prandtl number

1. K. N. Mehta, and K. N. Rao, *International Journal of Engineering Science* **32** (1994) 297-302.

2. J. P. Pascal, and H. Pascal, *International journal of non-linear mechanics* **30** (1995) 487-500.

3. N.E. Sabiri, and J. Comiti, *Chemical Engineering Science*, **50** (1995) 1193-1201.

4. A. Mansour, and N. Chigier, *Journal of Non-Newtonian Fluid Mechanics* **58** (1995) 161-194.

5. F. M. Hady, *Applied mathematics and computation* **68** (1995) 105-112.

6. S. Y. Sai, and T. H. Hsu, *Computers and Mathematics with Applications* **29** (1995) 99-108.

7. M. Pakdemirli, M. Yürüsoy, and A. Küçkbursa, *International journal of non-linear mechanics*, **31** (1996) 267-276.

8. J. Wu, and M. C. Thompson, *Journal of non-newtonian fluid mechanics*, **66** (1996) 127-144.

9. M. Kumari, I. Pop, and H. S. Takhar, *International journal of heat and fluid flow* **18** (1997) 625-631.

10. A. J. Chamkha, *International communications in heat and mass transfer*, **24** (1997) 643-652.

11. S. G. Etemad, *International communications in heat and mass transfer*, **24** (1997) 965-976.

12. S. Liu, and J. H. Masliyah, *Chemical Engineering Science* **53** (1998) 1175-1201.

13. M. G. Parvatiyar, *Journal of membrane science,* **148** (1998) 45-57.

14. H. I. Andersson, and O. A. Valnes, *Fluid dynamics research*, **24** (1999) 211-217.

15. J. W. Hoyt, *Some applications of non-newtonian fluid flow In Rheology Series* **8** (1999) 797-826

16. M. V. Papalexandris, *Combustion and Flame* **120** (2000) 526-538.

17. M. A. Hossain, M. S. Munir, and D. A. S. Rees, *International journal of thermal sciences* **39** (2000) 635-644.

18. I. Machač, B. Šiška, and R. Teichman, *Chemical Engineering and Processing: Process Intensification*, **41** (2002) 577-584.

19. G. C. Georgiou, *Journal of Non-Newtonian Fluid Mechanics*, **109** (2003) 93-114.

20. I. Machač, B. Šiška, and R. Teichman, *Chemical Engineering and Processing: Process Intensification* **41** (2002) 577-584.

21. R. Ellahi, M. M. Bhatti, A. Riaz, and M. Sheikholeslami, *Journal of Porous Media*, **17** (2002).

22. J. P. Hsu, S. H. Hung, and H. Y. Yu, *Journal of colloid and interface science*, **280** (2004) 256-263.

23. B. Siska, H. Bendova, and I. Machac, *Chemical engineering and processing*, **44** (2005) 1312-1319.

24. N. Ali and T. Hayat, *Applied Mathematics and Computation*, **193** (2007) 535-552.

25. D. Wang, and J. Bernsdorf, *Computers and Mathematics with Applications* **58** (2009) 1030-1034.

26. T. Hayat, N. Saleem, and N. Ali, *Communications in Nonlinear Science and Numerical Simulation*, **15** (2010) 2407-2423.

27. A. Hundertmark-Zaušková, and M. Lukáčová-Medvid'ová, *Computers and Mathematics with Applications* **60** (2010) 572-590.

28. B. Straughan, *International Journal of Heat and Mass Transfer* **53** (2010) 2808-2812.

29. B. Straughan, *Physics Letters A* **374** (2010) 2667-2669.

30. H. Al-Qahtani, and B. S. Yilbas, *Physica B: Condensed Matter*, **405** (2010) 3869-3874.

31. V. Tibullo and V. Zampoli, *Mechanics Research Communications*, **38** (2011) 77-79.

32. S. Han, L. Zheng, C. Li, and X. Zhang, *Applied Mathematics Letters*, **38** (2014) 87-93.

33. S. A. M. Haddad, *International Journal of Heat and Mass Transfer*, **68** (2014) 659-668.

34. I. S. Shivakumara, M. Ravisha, C. O. Ng, and V. L. Varun, *International Journal of Non-Linear Mechanics*, **71** (2015) 39-47.

35. M. Mustafa, J. A. Khan, T. Hayat, and A. Alsaedi, *Journal of Molecular Liquids* **211** (2015) 119-125.

36. T. Hayat, K. Muhammad, M. Farooq and A. Alsaedi, *Journal of Molecular Liquids* **220** (2016) 216-222.

37. T. Hayat, M. I. Khan, M. Farooq, T. Yasmeen, and A. Alsaedi, *Journal of Molecular Liquids* **220** (2016) 49-55.

38. S. Nadeem, and N. Muhammad, *Journal of Molecular Liquids*, **224** (2016) 423-430.

39. F. M. Abbasi, and S. A. Shehzad, *Journal of Molecular Liquids*, **220** (2016) 848-854.

40. J. R. Reddy, V. Sugunamma, and N. Sandeep, *Journal of Molecular Liquids*, **223** (2016) 1234-1241.

41. J. Li, L. Zheng, and L. Liu, *Journal of Molecular Liquids*, **221** (2016) 19-25.

42. M. Ramzan, M. Bilal, and J. D. Chung, *Journal of Molecular Liquids*, **223** (2016) 1284-1290.

43. R. Malik, M. Khan, and M. Mushtaq, *Journal of Molecular Liquids*, **222** (2016) 430-434.

44. Salahuddin, M. Y. Malik, A. Hussain, S. Bilal, and M. Awais, *Journal of magnetism and magnetic materials* **401** (2016) 991-997.

45. A. S. Dogonchi, and D. D. Ganji, *Journal of the Taiwan Institute of Chemical Engineers*, **80** (2017) 52-63.

46. S. M. Upadhya, C. S. K. Raju, and S. Saleem, *Results in Physics* **9** (2018) 779-786.

47. K. A. Kumar, J. R. Reddy, V. Sugunamma, and N. Sandeep, *Alexandria Engineering Journal* (2016).

48. M. A. Meraj, S. A. Shehzad, T. Hayat, F. M. Abbasi, and A. Alsaedi, *Applied Mathematics and Mechanics*, **38** (2017) 557-566.

49. S. M. Upadhya, C. S. K. Raju, S. A. Shehzad, and F. M. Abbasi, *Powder Technology* **340** (2018) 68-76.

50. P. D. Prasad, S. V. K. Varma, C. S. K. Raju, S. A. Shehzad, and M. A. Meraj, *Rev. Mex. Fis* **64** (2018) 519-529.

51. V. Nagendramma, C. S. K. Raju, B. Mallikarjuna, S. A. Shehzad, and A. Leelarathnam, *Applied Mathematics and Mechanics* **39** (2018) 623-638.

52. M. Khan, H. Sardar, and M. M. Gulzar, *Results in physics* **8** (2018) 524-531.